Journal of Alloys and Compounds 517 (2012) 20–25

Contents lists available at SciVerse ScienceDirect

Journal of Alloys and Compounds

journal homepage: www.elsevier.com/locate/jallcom

Effect of aluminum fluoride coating on the electrochemical and thermal properties of $0.5Li_2MnO_3 \cdot 0.5LiNi_{0.5}Co_{0.2}Mn_{0.3}O_2$ composite material

Jin-Hwa Kim [a,b], Min-Sik Park [a], Jun-Ho Song [a], Dong-Jin Byun [b], Young-Jun Kim [a], Jeom-Soo Kim [a,*]

[a] Advanced Batteries Research Center, Korea Electronics Technology Institute, Seongnam, Gyeonggi 463-816, Republic of Korea
[b] Department of Materials Science and Engineering, Korea University, Seoul 136-713, Republic of Korea

ARTICLE INFO

Article history:
Received 26 September 2011
Received in revised form
16 November 2011
Accepted 24 November 2011
Available online 2 December 2011

Keywords:
Aluminum fluoride
Cathode
Lithium ion battery
Oxide

ABSTRACT

The positive effect of AlF_3 (Al–F) coating on the over-lithiated transition metal oxide with a composition of $0.5Li_2MnO_3 \cdot 0.5LiNi_{0.5}Co_{0.2}Mn_{0.3}O_2$ has been investigated to address its potential use in lithium ion batteries. On the basis of various structural and electrochemical characterizations, we elucidate a correlation between surface structure and its electrochemical performance. After the controlled coating with AlF_3 (Al–F), we observed notable improvements on cyclic performance and rate capability as well as thermal stability. We found that uniformly introduced AlF_3 (Al–F) not only preserves the electrochemical kinetics at the surface of the oxide but also stabilizes its surface as a protective layer against electrolyte oxidation during the high voltage charging. Such improvements will provide a further progress on the development of high-capacity cathode materials fulfilled with the stringent safety requirements.

1. Introduction

Over the past decade, significant efforts have been devoted to explore low cost, high energy, and safe cathode materials for lithium-ion batteries (LIB). New cathode materials such as $LiMn_{0.5}Ni_{0.5}O_2$, $LiNi_{1/3}Co_{1/3}Mn_{1/3}O_2$, $LiFePO_4$, and $xLi_2M'O_3 \cdot (1-x)LiMO_2$ (M′ = Mn, Ti, Zr; M = Mn, Ni, Co) were successfully introduced to the LIB community as alternatives of $LiCoO_2$ [1–6]. Among them, $xLi_2M'O_3 \cdot (1-x)LiMO_2$ is being highlighted because it has the largest reversible capacity of more than 200 mAh g^{-1} and good thermal stability [6,7], which is directly related to the safety of battery. These high capacity and safety are the most competitive features, over conventional cathode materials such as $LiCoO_2$ and $LiMn_2O_4$, for use in automotive applications.

From a series of $xLi_2M'O_3 \cdot (1-x)LiMO_2$, $xLi_2MnO_3 \cdot (1-x)LiMO_2$ is most extensively investigated because Li_2MnO_3 is contributing to the reversible capacity after high voltage activation (above 4.4 V *vs.* Li/Li^+) [6–8]. The Li_2MnO_3 takes an important role to supply extra lithium to the layered component resulting in stabilizing the electrode structure at fully charged state [6]. During the first charge to 4.6 V (*vs.* Li/Li^+), electrochemical extraction of lithium from $xLi_2MnO_3 \cdot (1-x)LiMO_2$ occurs in two steps [9]. The first step, characterized by a sloping voltage profile is responsible for the lithium removal from the layered component, $LiMO_2$, accompanied with oxidation of M; the second step, characterized by relatively a flat voltage profile above 4.4 V (*vs.* Li/Li^+) is attributed to removal of lithium (as Li_2O) from the rock salt component, Li_2MnO_3, which induces electrochemical activity to it. The corresponding reactions can be represented ideally:

$$\text{Firststep}: LiMO_2 \rightarrow MO_2 + Li^+ + e^- \quad (1)$$

$$\text{Secondstep}: Li_2MnO_3 \rightarrow MnO_2 + 2Li^+ + \tfrac{1}{2}O_2 + 2e^- \quad (2)$$

It is a mandatory process for $xLi_2MnO_3 \cdot (1-x)LiMO_2$ to be charged above 4.6 V (*vs.* Li/Li^+) to deliver large discharge capacity of more than 200 mAh g^{-1}. This environment is highly oxidative that both components (MO_2 and MnO_2) result in oxygen loss at the particle surface inducing the damage of surface; oxidation of electrolyte also occurs under this condition. These factors are the major contributors for the $xLi_2MnO_3 \cdot (1-x)LiMO_2$ to have limitations in rate capability and cycle performances.

In this work, we have investigated the possibility of protecting the $xLi_2MnO_3 \cdot (1-x)LiMO_2$ particle surface with aluminum fluoride (Al–F) layer to overcome these limitations. It has been reported that the effect of AlF_3 coating on some cathode materials such as $LiCoO_2$, $LiNi_{1/3}Co_{1/3}Mn_{1/3}O_2$, and $LiMn_{0.5}Ni_{0.5}O_4$ [10–12]. However, the exact role of AlF_3 introduced on the surface of the materials has not been clearly identified yet.

Our intention to get benefits from Al–F coating is that (1) the Al–F/$xLi_2MnO_3 \cdot (1-x)LiMO_2$ interface comprised of Li–Al–F acts as a stable lithium conducting solid electrolyte, and (2) the main composition of coating layer, Al–F,

* Corresponding author. Tel.: +82 31 789 7491; fax: +82 31 789 7499.
E-mail address: js.energy@keti.re.kr (J.-S. Kim).

0925-8388/$ – see front matter © 2011 Elsevier B.V. All rights reserved.
doi:10.1016/j.jallcom.2011.11.117

might protect the surface of $xLi_2MnO_3\cdot(1-x)LiMO_2$ from the severe oxidation of electrolyte or the acid attack which both of them are known as possible contributors to the manganese solubility of $xLi_2MnO_3\cdot(1-x)LiMO_2$. We report our progress in increasing the rate capability, improving cycle life, stabilizing thermal stability; the results offer the possibility of designing lithium-ion conducting layer on the $xLi_2MnO_3\cdot(1-x)LiMO_2$ to protect an active material at high voltages.

2. Experimental

$xLi_2MnO_3\cdot(1-x)LiMO_2$ with a composition of $0.5Li_2MnO_3\cdot0.5LiNi_{0.5}Co_{0.2}Mn_{0.3}O_2$ was prepared by a co-precipitation method using metal sulfate precursors (Mn, Co, Ni) followed by sintering at 900 °C for 10 h under air atmosphere. Aluminum fluoride with a desired stoichiometry of AlF_3 was coated on the surface of $0.5Li_2MnO_3\cdot0.5LiNi_{0.5}Co_{0.2}Mn_{0.3}O_2$ powder through a wet coating process. Stoichiometric amounts of ammonium fluoride (NH_4F, Aldrich, 98%), and aluminum nitrate nonahydrate ($AlNO_3\cdot9H_2O$, Aldrich, 98%) were separately dissolved in distilled water. Firstly, the prepared powder was put into the $AlNO_3$ solution and constantly stirred at 25 °C for 1 h. After that, the NH_4F solution was slowly dropped into the solution containing the $0.5Li_2MnO_3\cdot0.5LiNi_{0.5}Co_{0.2}Mn_{0.3}O_2$ powder and stirred again at 80 °C for 5 h. After filtration, the obtained powder was dried in a vacuum oven at 60 °C for 12 h to completely remove the residual moisture and then finally sintered at 400 °C for 5 h under Ar atmosphere to avoid the formation of Al_2O_3. The nominal coating amount of AlF_3 was about 0.25 mol% of the parent material.

The morphology and microstructure of AlF_3 coated $0.5Li_2MnO_3\cdot0.5LiNi_{0.5}Co_{0.2}Mn_{0.3}O_2$ were examined by a field emission scanning electron microscope (FE-SEM, JEOL JSM-7000F) and powder X-ray diffraction (Empyrean, PANalytical, Netherlands). The chemical composition of Al–F coated $0.5Li_2MnO_3\cdot0.5LiNi_{0.5}Co_{0.2}Mn_{0.3}O_2$ was confirmed energy dispersive X-ray spectroscopy (EDS). The thermal stability for the AlF_3 coated $0.5Li_2MnO_3\cdot0.5LiNi_{0.5}Co_{0.2}Mn_{0.3}O_2$ was tested with a differential scanning calorimetric (DSC, METTLER TOLEDO STARe system) analysis after being charged to 4.6 V *vs.* Li/Li^+.

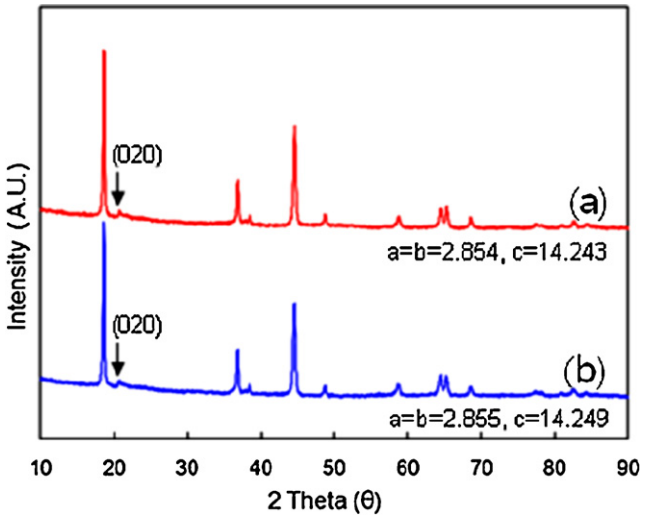

Fig. 1. Powder XRD patterns of (a) pristine $0.5Li_2MnO_3\cdot0.5LiNi_{0.5}Co_{0.2}Mn_{0.3}O_2$ and (b) Al–F coated $0.5Li_2MnO_3\cdot0.5LiNi_{0.5}Co_{0.2}Mn_{0.3}O_2$.

Coin-type (CR2032) half-cells were assembled to evaluate electrochemical properties of the AlF_3 coated $0.5Li_2MnO_3\cdot0.5LiNi_{0.5}Co_{0.2}Mn_{0.3}O_2$ powder. The electrode was prepared by a coating slurry containing active materials (90 wt%), conducting agent (Super-P, 5 wt%), and binder (PVdF, 5 wt%) dissolved in NMP (*N*-methyl-2-pyrrolidone) on Al foil current collector with a thickness of 15 °C. A porous polyethylene (PE) membrane was used as a separator and Li metal foil was used as counter and reference electrodes. 1.0 M $LiPF_6$ dissolved in ethylene carbonate (EC)/ethylmethyl carbonate (EMC) (1:2 vol., PANAX Etec Co. Ltd.) was used as an electrolyte. The cells were galvanostatically charged and discharged in a voltage range of 2.0–4.8 V *vs.* Li/Li^+. Cyclic voltammograms for the samples were obtained

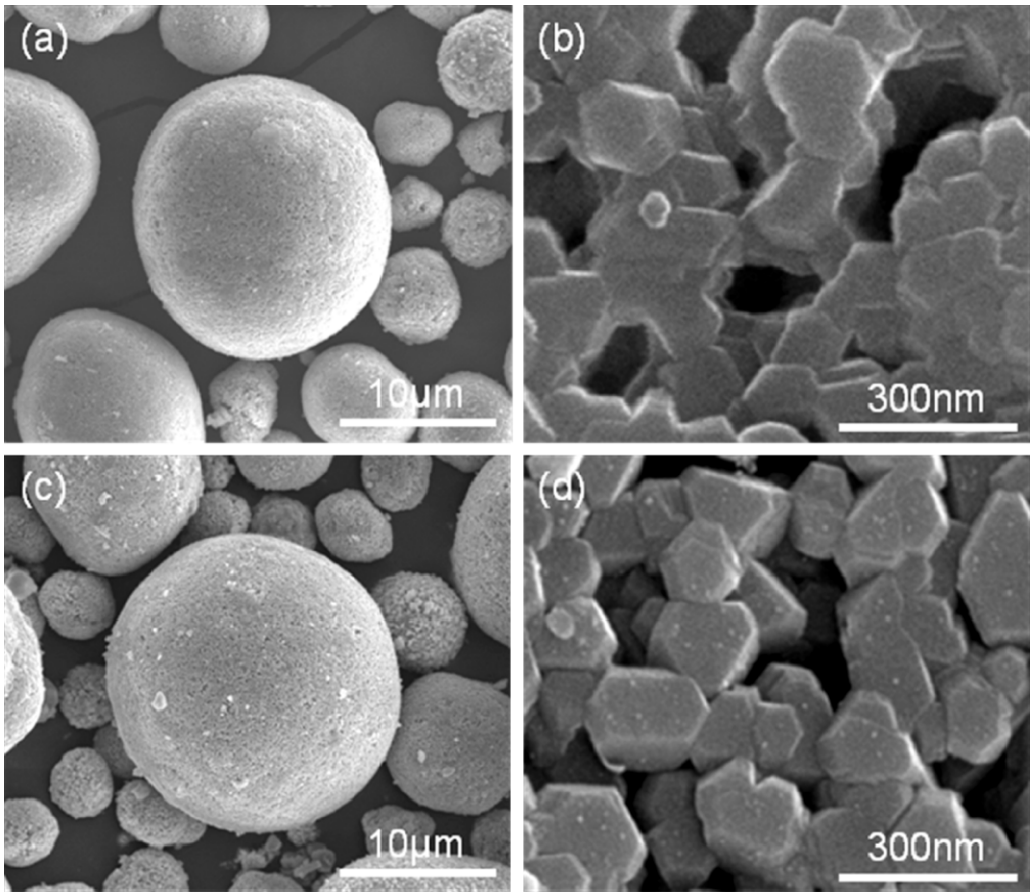

Fig. 2. FE-SEM images at different magnifications: (a) and (b) pristine $0.5Li_2MnO_3\cdot0.5LiNi_{0.5}Co_{0.2}Mn_{0.3}O_2$ and (c) and (d) Al–F coated $0.5Li_2MnO_3\cdot0.5LiNi_{0.5}Co_{0.2}Mn_{0.3}O_2$.

in a voltage range of 2.0–4.8 V *vs.* Li/Li^+ with a scan rate of 0.05 mV s^{-1}. AC-impedance measurements were performed using an electrochemical impedance analyzer (SP-300, Bio-Logic Ins.) over a frequency range from 1 MHz to 0.01 Hz with the amplitude of 10 mV.

3. Results and discussion

The powder XRD patterns of the pristine $0.5Li_2MnO_3{\cdot}0.5LiNi_{0.5}Co_{0.2}Mn_{0.3}O_2$, and Al–F coated materials are shown in Fig. 1a and b. The pristine sample (Fig. 1 a) shows a typical XRD pattern of $xLi_2MnO_3{\cdot}(1-x)LiMO_2$ materials with a characteristic (0 2 0) reflection at ~21° 2θ, which is representing the Li_2MnO_3-like component ($C2/m$) in the structure [5]. Because of the paucity of the data, the lattice information of samples was refined using the $R3{-}m$ (high symmetry), rather than the $C2/m$ (low symmetry). The pattern of Al–F coated sample is identical to the pristine sample and did not show any significant difference of lattice parameters (pristine $a = b = 2.854$, $c = 14.243$; Al–F coated $a = b = 2.855$, $c = 14.249$). There is no trace of Al–F compound in the XRD pattern of Al–F coated sample, which can be speculated for the low content of Al–F and/or the amorphous phase of coated Al–F.

Fig. 2 shows FE-SEM images of pristine and Al–F coated samples at different magnifications. Both samples have a spherical shape with an average particle size (D50) of about 12 μm with much smaller primary particle (a few hundreds nm) whether the sample was coated or not. The pristine sample has smooth surfaces while the coating material, Al–F nanoparticles, was observed on the surface of Al–F coated sample, as shown Fig. 2b and d, respectively.

To verify the coating homogeneity and surface chemistry, element mapping with energy-dispersive X-ray spectroscopy (EDX) was applied to the Al–F coated sample. The existence of Al and F on the surface of Al–F coated sample was confirmed by EDX dot mapping in Fig. 3. According to element mapping results, even distribution of Al and F was clearly observed on the surface of the Al–F coated sample. It is evident that the $0.5Li_2MnO_3{\cdot}0.5LiNi_{0.5}Co_{0.2}Mn_{0.3}O_2$ is successfully covered by the amorphous Al–F compound.

Electrochemical reactivity of the pristine (a) and Al–F coated sample (b) was compared to determine the effect of Al–F coating on the electrochemical properties of $0.5Li_2MnO_3{\cdot}0.5LiNi_{0.5}Co_{0.2}Mn_{0.3}O_2$ in Fig. 4. The cyclic voltammetry was measured with a scan rate of 0.05 mV s^{-1} in the voltage range of 2.0–4.8 V *vs.* Li/Li^+. The pristine sample shows the characteristic cyclic voltammogram of the $xLi_2M'O_3{\cdot}(1-x)LiMO_2$ type materials, which has a large oxidation peak around 4.6 V in Fig. 6a. This peak is corresponding to the extraction of lithium from transition metal layer majorly. More than four redox couples were observed for the pristine and Al–F coated samples each. In the case of Al–F coated sample, the shape of oxidation peak around 4.6 V is much sharper than the one of pristine sample. The Al–F coated sample has a similar specific current level ($\Delta \sim 0.006$ A g^{-1}) at both start (4.3 V) and end (4.8 V) points while the pristine one has a larger current difference ($\Delta \sim 0.032$ A g^{-1}) at the same points in the 4.6 V reaction region. This indicates that the oxidation reaction (~4.6 V) of the Al–F coated sample is almost fully carried out compared to the pristine sample, which was interrupted by experimental conditions. During the oxidation above 4.6 V, lithium of Li_2MnO_3 is extracted and MnO_2 is formed as a consequence. It has been reported that MnO_2 has electrochemical reactivity with lithium in the voltage range between 2.0 and 3.0 V [6]. The redox couple shown around 3.0 V is the proof of the formation of MnO_2 in Fig. 5b. That couple is clearly observed for the Al–F coated sample (Fig. 5b) but it is hard to find for the pristine sample. For the pristine one (Fig. 5a), it looks like that the oxidation peak is merged to

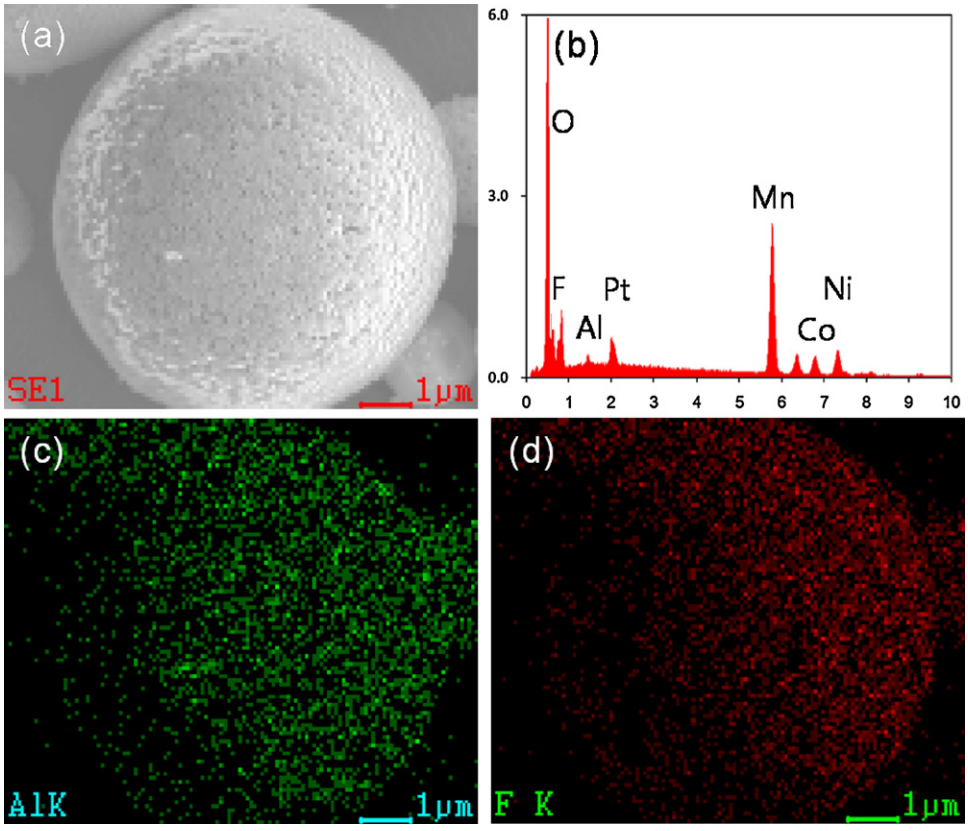

Fig. 3. Element mapping results obtained from energy dispersive X-ray spectroscopy (EDX) for Al–F coated $0.5Li_2MnO_3{\cdot}0.5LiNi_{0.5}Co_{0.2}Mn_{0.3}O_2$ powder: (a) SEM image, (b) EDS profile, (c) Al K, and (d) F K.

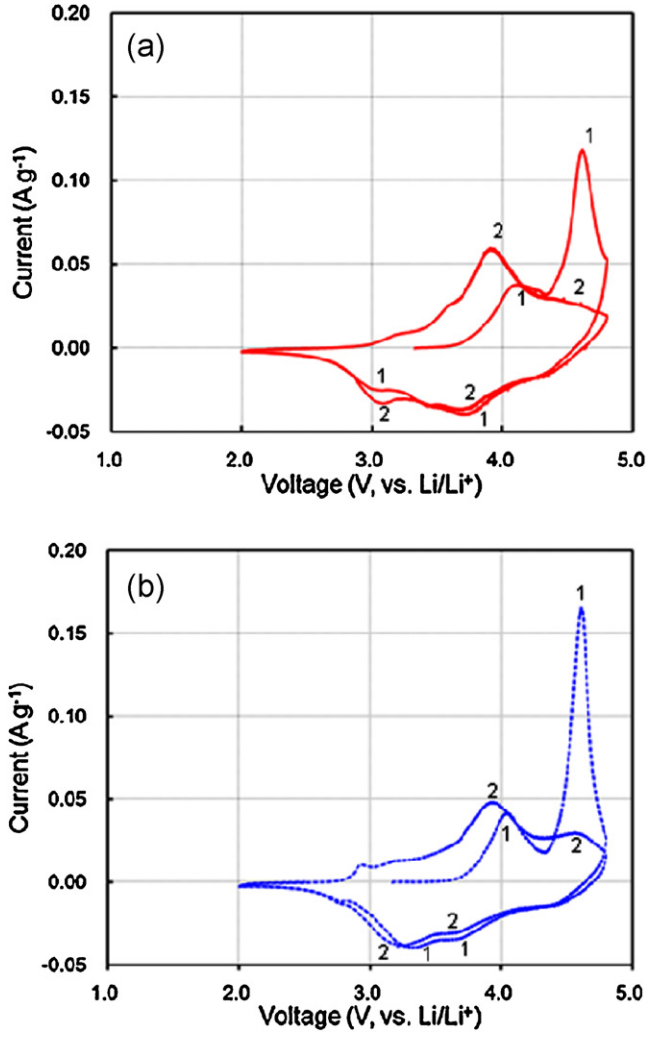

Fig. 4. Cyclic voltammetry of (a) pristine $0.5Li_2MnO_3{\cdot}0.5LiNi_{0.5}Co_{0.2}Mn_{0.3}O_2$ and (b) Al–F coated $0.5Li_2MnO_3{\cdot}0.5LiNi_{0.5}Co_{0.2}Mn_{0.3}O_2$; scan rate was fixed at 0.05 mV s^{-1} in a voltage range of 2.0–4.8 V *vs.* Li/Li^+.

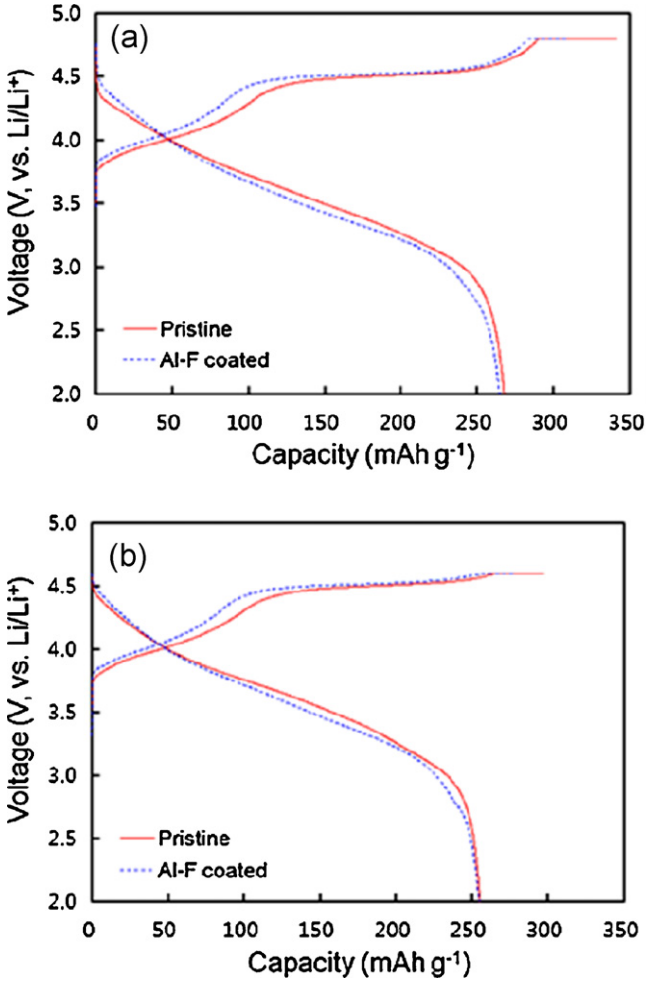

Fig. 5. Comparisons of galvanostatic charge and discharge profiles at the first cycle for pristine and Al–F treated $0.5Li_2MnO_3{\cdot}0.5LiNi_{0.5}Co_{0.2}Mn_{0.3}O_2$ electrodes: (a) 4.8 V *vs.* Li/Li^+ charge cut-off and (b) 4.6 V *vs.* Li/Li^+ charge cut-off.

higher voltage one around 3.2 V while the reduction peak is buried in the one around 2.7 V. These results imply indirectly that the surface coating using the Al–F compound could effectively improve the electrochemical kinetic of $0.5Li_2MnO_3{\cdot}0.5LiNi_{0.5}Co_{0.2}Mn_{0.3}O_2$.

The voltage profiles of the initial charge/discharge cycle of the half cells with the pristine and Al–F coated $0.5Li_2MnO_3{\cdot}0.5LiNi_{0.5}Co_{0.2}Mn_{0.3}O_2$ cathodes were measured with the voltage range of 2.0–4.6 V *vs.* Li/Li^+ at 0.1 C rate (0.18 mA cm^{-2}, 25 mA g^{-1}) as shown in Fig. 5. The applied charging condition was a constant current followed by a constant voltage (CC–CV) to ensure the full reaction at desired voltage (4.6 V). The initial charge profiles of the cells show a typical behavior of $Li_2M'O_3{\cdot}(1-x)LiMO_2$ type materials, indicating lithium extraction first from the layered component ($LiNi_{0.5}Co_{0.2}Mn_{0.3}O_2$) between 3.0 and 4.35 V, followed by further lithium extraction from the rock salt component (Li_2MnO_3) and oxygen loss up to 4.6 V. Even though the pristine electrode exhibits higher charge capacity (~295 mAh g^{-1}) than Al–F coated electrode (~280 mAh g^{-1}), both electrodes deliver similar capacity (~255 mAh g^{-1}) on following discharge. The Al–F coated electrode provides a higher coulombic efficiency of 91% compared to the pristine electrode (86%). There are a couple of reports to claim improving the coulombic efficiency by surface coating with $AlPO_4$ [13] and Li–Ni–PO_4 [14], but the values of efficiency were less than 90% for both cases. By contrast, the Al–F coated electrodes showed more than 90% coulombic efficiency (91%) while keeping the same discharge capacity as the pristine electrode. Because the discharge capacity of the pristine and Al–F coated electrodes is same, the difference of charge capacity governs the cycling efficiency in the cells. It is noticeable that the pristine electrode has a longer CV region at 4.6 V than the Al–F coated one have, indicating that the pristine electrode needs a longer time to reach the equilibrium under the same conditions. The low electrochemical kinetics and side reactions with electrolyte might be the possible reasons for the longer CV region, which contributes to the low coulombic efficiency of pristine electrode directly. Unlike the pristine electrode, the Al–F coated electrode reaches the equilibrium in a shorter time represented by shorter CV region. This result reveals that the Al–F coating is effective to protect the surface of $0.5Li_2MnO_3{\cdot}0.5LiNi_{0.5}Co_{0.2}Mn_{0.3}O_2$ from side reactions with electrolyte and/or to enhance its electrochemical kinetics. Fig. 6 presents the discharge capacity *vs.* cycle number of the pristine and Al–F coated electrodes with a constant current of 0.5 C (0.90 mA cm^{-2}, 125 mA g^{-1}) in a voltage range of 2.0–4.6 V *vs.* Li/Li^+ at room temperature. The cells were pre-conditioned with a current of 0.1 C for 2 cycles under the same voltage range prior to cycle test. The Al–F coated electrode shows excellent capacity retention after 50 cycles. The pristine electrode had an initial discharge capacity (0.5 C) of 205.9 mAh g^{-1} and retained its initial capacity of approximately 93% at the 50th cycle. Meanwhile, the Al–F coated one had a higher initial capacity (216.2 mAh g^{-1}) and

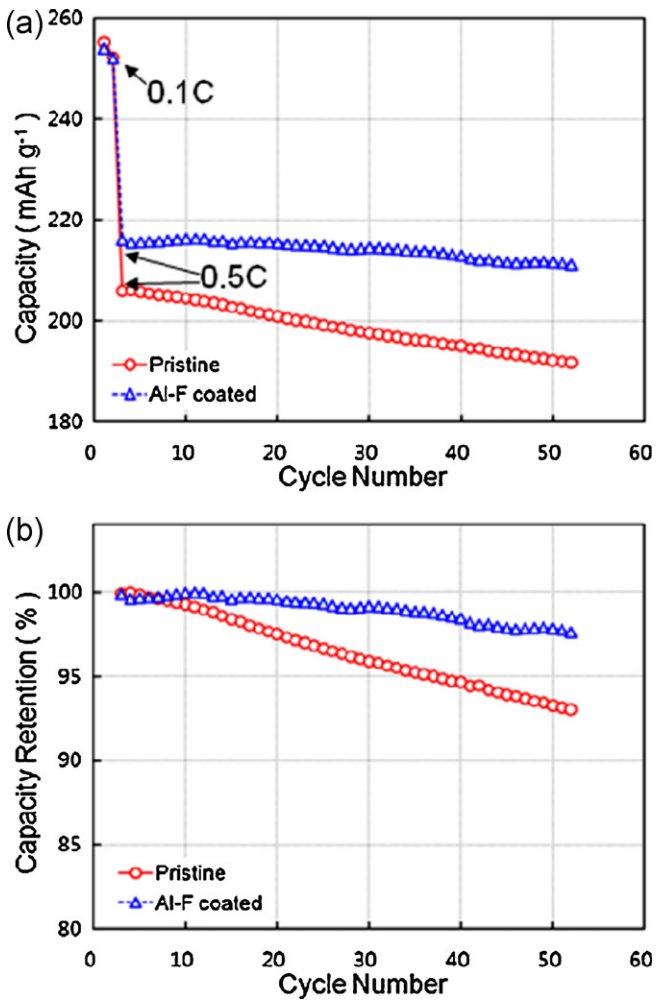

Fig. 6. Cycle performances of pristine and Al–F treated $0.5Li_2MnO_3{\cdot}0.5LiNi_{0.5}Co_{0.2}Mn_{0.3}O_2$ electrodes during 50 cycles: (a) discharge capacity and (b) capacity retention; the cells charged and discharged with a constant current of 125 mA g^{-1} (0.5 C) in a voltage range of 2.0–4.6 *vs.* Li/Li^+.

improved capacity retention, exhibiting 98% of the initial discharge capacity at the 50th cycle.

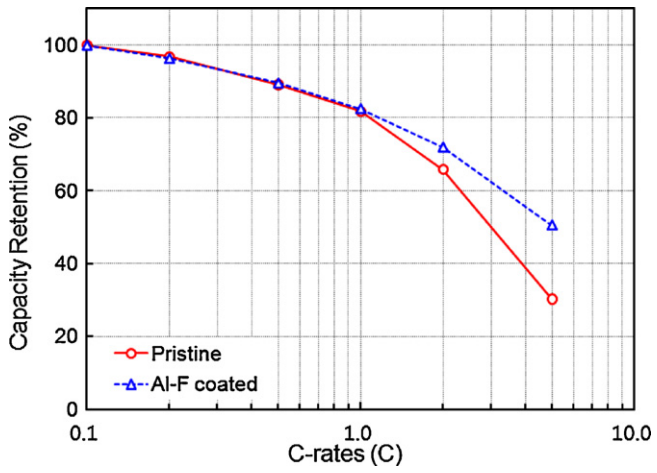

Fig. 7. A comparison of rate capability for pristine and Al–F treated $0.5Li_2MnO_3{\cdot}0.5LiNi_{0.5}Co_{0.2}Mn_{0.3}O_2$ electrodes at various discharge C rates (0.1–5.0 C) with fixed charge rate of 0.2 C.

Fig. 7 shows the discharge capacity of the pristine and Al–F coated electrodes at various currents (C-rates) in a voltage range of 2.0–4.6 V *vs.* Li/Li^+. According to the comparison of rate capability, both the pristine and Al–F coated electrodes have similar capacity retention up to 1.0 C (1.80 mA cm^{-2}, 250 mA g^{-1}). However, the Al–F coated electrode exhibits better discharge-capacity retention than pristine one beyond 1.0 C. The difference of capacity retention is increased to 20% at 5.0 C which was close to 5% at 2.0 C. Based on these electrochemical measurements, we note that the Al–F coating on the surface of $0.5Li_2MnO_3{\cdot}0.5LiNi_{0.5}Co_{0.2}Mn_{0.3}O_2$ is substantially effective to enhance coulombic efficiency, cycle performance, and rate capability. The HF can be generated from the result of reactions between water and $LiPF_6$ salt. Less than a few tens of ppm level of water is enough to initiate this reaction in the electrolyte. The generated HF attacks the active materials causing the degradation of cycling performance [15]. The decomposition of $LiPF_6$ produces LiF as a byproduct which precipitates on the surface of the electrode. These precipitates, electronically insulator, result in poor rate capability. While the pristine electrode is not free from HF attack, the Al–F coated electrode has an Al–F protection layer on the surface. It is speculated that the Al–F coating could improve the charge transfer resistance of an electrode, which facilitates Li^+ insertion/deinsertion at the interface. The amorphous Li–Al–F can possibly be formed in between the Al–F and the $0.5Li_2MnO_3{\cdot}0.5LiNi_{0.5}Co_{0.2}Mn_{0.3}O_2$ during the heat treatment after coating. Meanwhile the Al–F (AlF_3) is not a good lithium ion conductor, Li–Al–F compounds such as $LiAlF_4$, have been reported as a good lithium ion conductor having an ionic conductivity value of 1×10^{-4} S m^{-1} [16]. While outer layer Al–F may protect the pristine material from the HF attack, the inner layer Li–Al–F is attributed to improve rate capability.

To correlate the improvement of electrochemical properties with interfacial impedance at the interface between the cathode and electrolyte, electrochemical impedance spectroscopy (EIS) was performed in the pristine and Al–F coated $0.5Li_2MnO_3{\cdot}0.5LiNi_{0.5}Co_{0.2}Mn_{0.3}O_2$ electrode after fully being charged to 4.6 V (*vs.* Li/Li^+) as shown in Fig. 8. The Nyquist plots for both electrodes present two semicircles, one in the high-to-medium frequency region and the other in the low frequency region. The first semicircle is attributed the resistance of the surface film and the second one is attributed to the charge-transfer resistance [17]. After the Al–F coating, we found that the charge transfer resistance is notably reduced by the Al–F coating. It

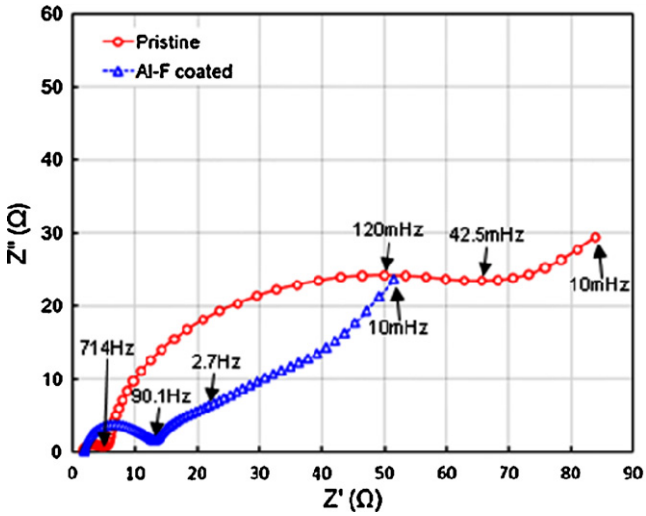

Fig. 8. Electrochemical impedance spectra (EIS) of pristine and Al–F coated cathode being charged to 4.6 V *vs.* Li/Li^+ at the first cycle.

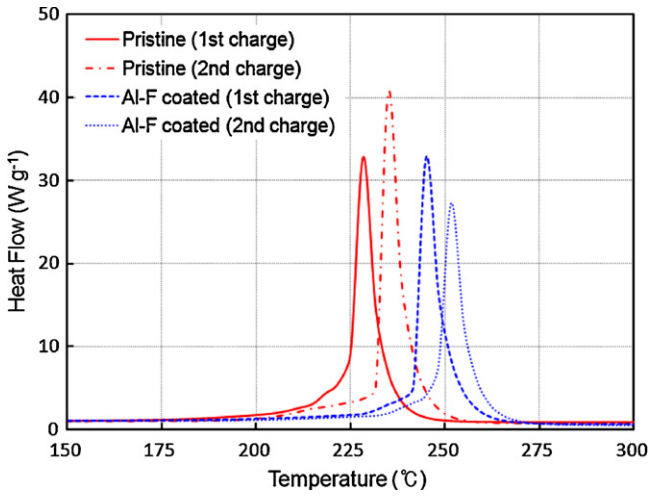

Fig. 9. Differential scanning calorimetry (DSC) traces of (a) pristine $0.5Li_2MnO_3{\cdot}0.5LiNi_{0.5}Co_{0.2}Mn_{0.3}O_2$ electrodes and (b) Al–F coated $0.5Li_2MnO_3{\cdot}0.5LiNi_{0.5}Co_{0.2}Mn_{0.3}O_2$ electrodes after being charged to 4.6 V *vs.* Li/Li^+.

seems to supports that lithium conducting Li–Al–F compounds could be formed as a part of Al–F coating layer on the surface of $0.5Li_2MnO_3{\cdot}0.5LiNi_{0.5}Co_{0.2}Mn_{0.3}O_2$, which could facilitate lithium-ion conduction by reducing charge-transfer resistance.

On the other hand, it is important to measure the thermal stability, especially at delithiated (charged) state, because the thermal stability of cathode materials is closely related to battery safety. Enhancement of thermal stability is another important feature of Al–F coating on $0.5Li_2MnO_3{\cdot}0.5LiNi_{0.5}Co_{0.2}Mn_{0.3}O_2$ as shown in Fig. 9. Each of the pristine and Al–F coated electrodes was charged to 4.6 V prior to test with differential scanning calorimetry (DSC). DSC profiles of the both electrodes were compared after the first charge and second charge, respectively. Most of previous studies were focused on the stability of electrode only after the first charge [18–20]. We have studied the change of thermal stability under different cycled condition since the surface and bulk chemistry of $0.5Li_2MnO_3{\cdot}0.5LiNi_{0.5}Co_{0.2}Mn_{0.3}O_2$ is changed after the first charge. For the first charge, the pristine electrode shows a major exothermic peak at 235 °C with an onset of decomposition temperature around 192 °C and a heat generation of 1427 J g^{-1}. Meanwhile, the Al–F coated one exhibits a relatively reduced peak at 252 °C with an onset temperature of 232 °C and a heat generation of 1398 J g^{-1}. In the case of second charge, the peaks are shifted to higher temperature by 7 °C for both electrodes. The heat generation of the pristine electrode is 1440 J g^{-1} and the Al–F coated electrode has a heat generation of 1405 J g^{-1}. This result implies that the Al–F coating is effective to control the decomposition temperature of the material proved by increasing the peak position while the bulk stability is not affected by the surface coating indicated by relatively similar total heat generation for all cases (~1400 J g^{-1}). In the second charge, the peak shifting to high temperature indicates improved thermal stability over the first charge in general. Except peak position and heat generation, the shape of peak that is presented by a maximum heat flow and sharpness is another indicator of thermal stability. With this point of view, we agree that the Al–F coated electrode with a reduced maximum heat flow has better thermal stability than the pristine electrode. Thus, there are some changes in the thermal stability of $0.5Li_2MnO_3{\cdot}0.5LiNi_{0.5}Co_{0.2}Mn_{0.3}O_2$ after the first charge. Therefore, it is necessary to conduct DSC test in first and second charge in turns to investigate the thermal stability of $xLi_2MnO_3{\cdot}(1-x)LiMO_2$ type materials precisely. Improved thermal stability of the Al–F coated electrode is resulted from the Al–F layer on the surface of $0.5Li_2MnO_3{\cdot}0.5LiNi_{0.5}Co_{0.2}Mn_{0.3}O_2$. It is reasonable to assume that the main portion of Al–F compounds is the AlF_3 since the stoichiometry of AlF_3 was applied for Al–F coating. Among the Al–F compounds, AlF_3 has a high melting point of 1291 °C which may contribute to enhance thermal stability of the Al–F coated electrode. Furthermore, the AlF_3 layer prevents the highly unstable oxidized positive electrode particle from direct contact with the electrolyte solution, thereby, reducing the exothermic reaction.

4. Conclusions

$0.5Li_2MnO_3{\cdot}0.5LiNi_{0.5}Co_{0.2}Mn_{0.3}O_2$ particles were uniformly coated with an Al–F layer. Surface modified $0.5Li_2MnO_3{\cdot}0.5LiNi_{0.5}Co_{0.2}Mn_{0.3}O_2$ with aluminum fluoride (Al–F) exhibits significantly improved cycle performance, rate capability, and thermal stability. The capacity retention of Al–F coated pristine was estimated to be 98% after 50 cycles, while that of the pristine was 93% within a voltage range of 2.0–4.6 V *vs.* Li/Li^+. For the rate capability, the Al–F coated sample exhibits better discharge-capacity retention of 50% than pristine (30%) at 5.0 C. Effective Al–F coating is attributed to the surface protection of pristine sample from the chemical attack resulting enhanced coulombic efficiency and cycle performance. It is speculated that the amorphous Li–Al–F layer, possibly formed in between Al–F and $0.5Li_2MnO_3{\cdot}0.5LiNi_{0.5}Co_{0.2}Mn_{0.3}O_2$, may contribute to improve high rate capability. Additionally, Al–F coating provides better thermal stability to the pristine sample by shifting the decomposition temperature to about 20 °C higher. The surface modification of the $0.5Li_2MnO_3{\cdot}0.5LiNi_{0.5}Co_{0.2}Mn_{0.3}O_2$ using Al–F is a promising approach to improve the electrochemical properties and thermal stability.

Acknowledgement

This research was supported by a grant from the Fundamental R&D Program for Technology of World Premier Materials funded by the Ministry of Knowledge Economy, Republic of Korea (10037921).

References

[1] T. Ohzuku, Y. Makimura, Chem. Lett. 30 (2001) 744–745.
[2] S.B. Schougaard, J. Breger, M. Jiang, C.P. Grey, J.B. Goodenough, Adv. Mater. 18 (2006) 905–909.
[3] N. Yabuuchi, T. Ohzuku, J. Power Sources 171 (2003) 119–121.
[4] A.K. Padhi, K.S. Najundaswamy, J.B. Goodenough, J. Electrochem. Soc. 144 (1997) 1188–1194.
[5] J.-S. Kim, C.S Johnson, M.M Thackeray, Electrochem. Commun. 4 (2002) 205–209.
[6] M.M. Thackeray, C.S Johnson, J.T. Vaughey, N. Li, S.A. Hackney, J. Mater. Chem. 15 (2005) 2257–2267.
[7] C.S Johnson, N. Li, C. Lefief, J.T. Vaughey, M.M. Thackeray, Chem. Mater. 20 (2008) 6095–6106.
[8] M.M. Thackeray, S.-H. Kang, C.S Johnson, J.T. Vaughey, R. Benedek, S.A. Hackney, J. Mater. Chem. 17 (2007) 3112–3125.
[9] A.R. Armstrong, M. Holzapfel, P. Novak, C.S Johnson, S.-H. Kang, M.M. Thackeray, P.G. Bruce, J. Am. Chem. Soc. 128 (2006) 8694–8698.
[10] Y.-K. Sun, J.-M. Han, S.-T. Myung, S.-W. Lee, K. Amine, Electrochem. Commun. 8 (2006) 821–826.
[11] B.-C. Park, H.-B. Kim, S.-T. Myung, K. Amine, I. Belharouak, S.-M. Lee, Y.-K. Sun, J. Power Sources 178 (2008) 826–831.
[12] H. Lin, J. Zheng, Y. Yang, Mater. Chem. Phys. 119 (2010) 519–523.
[13] Y. Wu, A.V. Murugan, A. Manthiram, J. Electrochem. Soc. 155 (2008) A635–A641.
[14] S.-H. Kang, M.M. Thackeray, Electrochem. Commun. 11 (2009) 748–751.
[15] D.-J. Lee, K.-S. Lee, S.-T. Myung, H. Yashiro, Y.-K. Sun, J. Power Sources 196 (2011) 1353–1357.
[16] T. Oi, K. Miyauchi, K. Uehara, J. Appl. Phys. 53 (1982) 1823.
[17] S. Seki, Y. Kobayashi, H. Miyashiro, A. Yamanaka, Y. Mita, T. Iwahori, J. Power Sources 146 (2005) 741–744.
[18] Z. Lu, D.D. MacNeil, J.R. Dahn, Electrochem. Solid-State Lett. 4 (2001) A191–A194.
[19] K.-S. Lee, S.-T. Myung, D.-W. Kim, Y.-K. Sun, J. Power Sources 196 (2011) 6974–6977.
[20] Y.-K. Sun, S.-W. Cho, S.-T. Myung, K. Amine, J. Prakash, Electrochim. Acta 53 (2007) 1013–1019.